International Journal on Advanced Science Engineering Information Technology

Vol.12 (2022) No. 3
ISSN: 2088-5334

Tree Height Derivation under Homogeneous Tree Pattern by Segmentation Algorithm

Suzanah Abdullah [a], Mohd Fadzil Abdul Rashid [a], Muhammad Ariffin Osoman [b], Khairul Nizam Tahar [c,*]

[a] *Department of Built Environment Studies and Technologies, Faculty Architecture, Planning and Surveying, Universiti Teknologi MARA Perak Branch, 32610, Seri Iskandar, Perak, Malaysia*
[b] *Geoinfo Services Sdn Bhd, No 30 Jalan Bandar 2, Taman Melawati, Kuala Lumpur, Malaysia*
[c] *Centre of Studies for Surveying Science and Geomatics, Faculty of Architecture Planning and Surveying, Universiti Teknologi MARA, 40450 Shah Alam, Selangor, MALAYSIA*

*Corresponding author: *khairul0127@uitm.edu.my*

***Abstract*— Tree height is an important element in plantation areas to determine the tree's maturity for harvesting. Airborne Laser Scanning (ALS) technology can give accurate elevation using point cloud data. However, this technology is quite expensive and unsuitable for small areas and low-budget projects. This research focuses on the UAV technology, exploring the appropriate methods of determining a tree height from the UAV's photogrammetry images. This research aims to evaluate the tree height from the delineation of the tree crown. Three different algorithms have been used in this research to delineate tree crowns. The delineate tree crowns were extracted in vector format, and the crowns were used to calculate the tree height using the specific formula. The results of tree heights were assessed using Residual Mean Square Error (RMSE) to determine the accuracy of the outcome. It was found that the OBIA algorithm gives the best accuracy among these three algorithms. It is followed by WS algorithm and then IWS algorithm. The OBIA algorithm can give an accuracy of about 0.444m at 40m and 0.381m for 60 altitude. The accuracy for WS and OBIA stated that the 60m altitude gives the better accuracy compared to 40m altitude. However, the IWS gives the vice versa result. This research could help the planters to manage their plantations for the harvesting process.**

***Keywords*— Aerial mapping; segmentation; tree crown; tree height; accuracy.**

Manuscript received 18 Jun. 2021; revised 9 Sep. 2021; accepted 9 Dec. 2021. Date of publication 30 Jun. 2022.

I. Introduction

As mentioned in the literature, an accurate estimation of a tree height is critical for the forest ecosystem [1], that is, to ensure the effectiveness in forest management [2], and it is a high demand for forest structural information [3]. Tree height is defined as the vertical distance between two horizontal planes: one plane passing through the highest twig and the other through the base of the tree at mid-slope but is not synonymous with trunk length [4]. According to Barnes et al. [5], a tree height has been a critical element of forest inventory appraisal for decades, and it is required before the forest management plan is produced [6]. This is important to identify the forest condition in case of infection [7], determine forest stand attributes [8], tree stem mapping [9], and essential elements for estimating the global carbon cycle volume of a tree [10].

There are different methods and platforms used to estimate the tree heights from the terrain as well as the techniques for measuring a tree height that was developed long ago [11]. A number of different methods are used to measure tree heights from the ground. Previous research by Koeva et al. [12] explained that measuring tape is the most appropriate and accurate tool to measure tree height, but it is not a practical option for evaluation and forest monitoring. Like telescoping height measuring pole, the simplest method is easy to learn but limited to relatively small trees below 10m in height and requires more than one person to measure the treetop [13]. It is possible to apply a similar methodology to larger trees, but only by having a technician climb the tree (or an adjacent structure). This approach is used to measure potentially record-breaking trees but is obviously very slow and potentially dangerous and thus not suitable for measuring large numbers of trees in inventories. Over the years, the satellite image has been conventionally used for geospatial data collection [14] and has been increasingly used for evaluating forest information [15].

According to Tahar et al. [16], remote sensing technology is highly accurate and most commonly used to calculate tree canopy and individual trees' height. The satellite imaging platform is extremely advantageous in data acquisition for applications such as mining for fire detection, estimating forest parameters, forest inventory, vegetation height in ecological, offshore mapping, wetlands cover, and others. Many earlier researchers conducted research to determine tree height using satellite imagery [17], [18]. The sensor's accuracy depends on the resolution and the pixel-sized data acquired along the track.

Apart from the traditional method mentioned earlier, LiDAR is the best technology to model the forest structure and important for forest inventory methods. According to. Zhuo et al. [19] have studied the technique of determining tree height using LiDAR, but this technology is not extensively used in practice due to a problem assumed in various forest areas, especially in a dense forest. The accuracy of LiDAR is based on the characteristic of the sensor used and the site condition. The information on tree height would be useful to calculate biomass, estimate tree carbon stocks, and various forest structures. However, this technology overcomes most limitations as it can extract individual tree attributes such as tree location, the volume of canopy geometry, and canopy cover. Moreover, the LiDAR approach requires a high-cost survey for short flight sessions with experienced personnel. Manned aircraft is the best choice to cover a lot of areas very quickly and carry a heavy sensor due to much greater endurance.

The previous research has been using the Airborne Laser Scanning (ALS) technology, giving the accuracy of 3-10cm elevation to delineate the individual tree for diseased detection. Colefax et al. [20] investigated the tree height estimation using ALS and found that it is more reliable to estimate tree height for a taller stand condition. However, ALS structures are usually thought to underestimate tree heights because of the chances that treetops are lacking for different reasons. The spatial resolution of photogrammetry is derived from manned aircraft's data captured which is not usually accurate enough to produce good detection results. Meanwhile, ALS data provide coverage to a restricted spatial extent, repeatability, very expensive, and required labor demanding.

By considering these circumstances, this research focuses on the UAV technology, exploring the appropriate methods of determining a tree height from the UAV's photogrammetry images. The following discussions focus on tree height estimation methods based on a tree crown as suggested in literature. Technological evolution allows topographical aerial surveys to be available through UAV. UAV is emerging as a new image acquisition platform and offers an alternative to conventional image acquisition for both aerial and terrestrial photogrammetry [24]. Furthermore, due to logistical and functional limitations of manned aerial technologies, several studies have suggested that UAV can deliver efficiently and quality data. UAV flight missions provide high operational flexibility in terms of costs, place, platforms, time, and repeatability than satellite-based operations or traditional manned photogrammetric surveys. For these reasons, UAVs are highly complementary to traditional remote sensing platforms and have the potential to replace certain measurements that are conventionally acquired by satellites, crewed aircraft, or employing direct ground-based surveying.

II. Material and Method

In this research, the methodology process is divided into five main stages: exploratory research, data acquisition, data processing, results (DTM generation), and further analysis of the accuracy of the produced DTM. Fig. 1 illustrates the research methodology to determine tree height using UAV images. Stage one is about data acquisition for both the simulation and plantation areas. Stage two is about data processing, and stage three covers the results and accuracy assessment of tree height.

A. Data Acquisition

The experiments were conducted in two different approaches: single oil palm tree and oil palm tree plantation area. The research area was located at FELCRA (Federal Land Consolidation and Rehabilitation Authority) Nasaruddin Belia Berhad, Bota, Perak at a latitude 4°24'15.64"N and longitude 100°55'46.98"E. The area selected has a tree height of approximately 10 to 13 meters. According to the senior plantation officer, the tree height of oil palm is based on the crown's age, size, color, and shape. The size of the site research area is 200 meters by 200 meters in an oil palm plantation area.

The DJI 4 pro UAV is the main hardware used in this research. The use of DJI 4 Pro UAV, which includes a controller, battery, and iPad, was used as an image acquisition platform in this research. The Global Positioning System (GPS) equipment is used to establish the Ground Control Point (GCP) for the base and rover point around the plantation area. The set of Topcon total stations (total station, mini prism, tripod) is used to obtain the data of x, y, and z points for a detailed survey in the oil palm area, which is to validate and compare with the data acquired from UAV imagery. Meanwhile, hardware such as a high-end laptop is used in data processing to process the UAV images and perform data analysis.

Many software has been identified for this research concerning the multi-stages involved. This research applied the DJI Ground Station Pro to acquire images during flight planning at the image acquisition stage. This software is an iPad application created to control the flight by acquiring data autonomously. DJI Ground Station Pro or DJI GS Pro is an iPad application that conducts automated flight missions. After setting up the required flight zone and camera parameters, this research used DJI GS Pro to perform the efficient flight path. The Agisoft Photoscan software was used to process raw images and then the images were applied for analysis. Agisoft Photoscan software was applied to process the raw image derived from UAV imagery. The System for Automated Geoscientific Analyses (SAGA) and ArcMap software were implemented during the data processing stage. The selection of this software was based on the capabilities in image processing and the accessibility in data analysis.

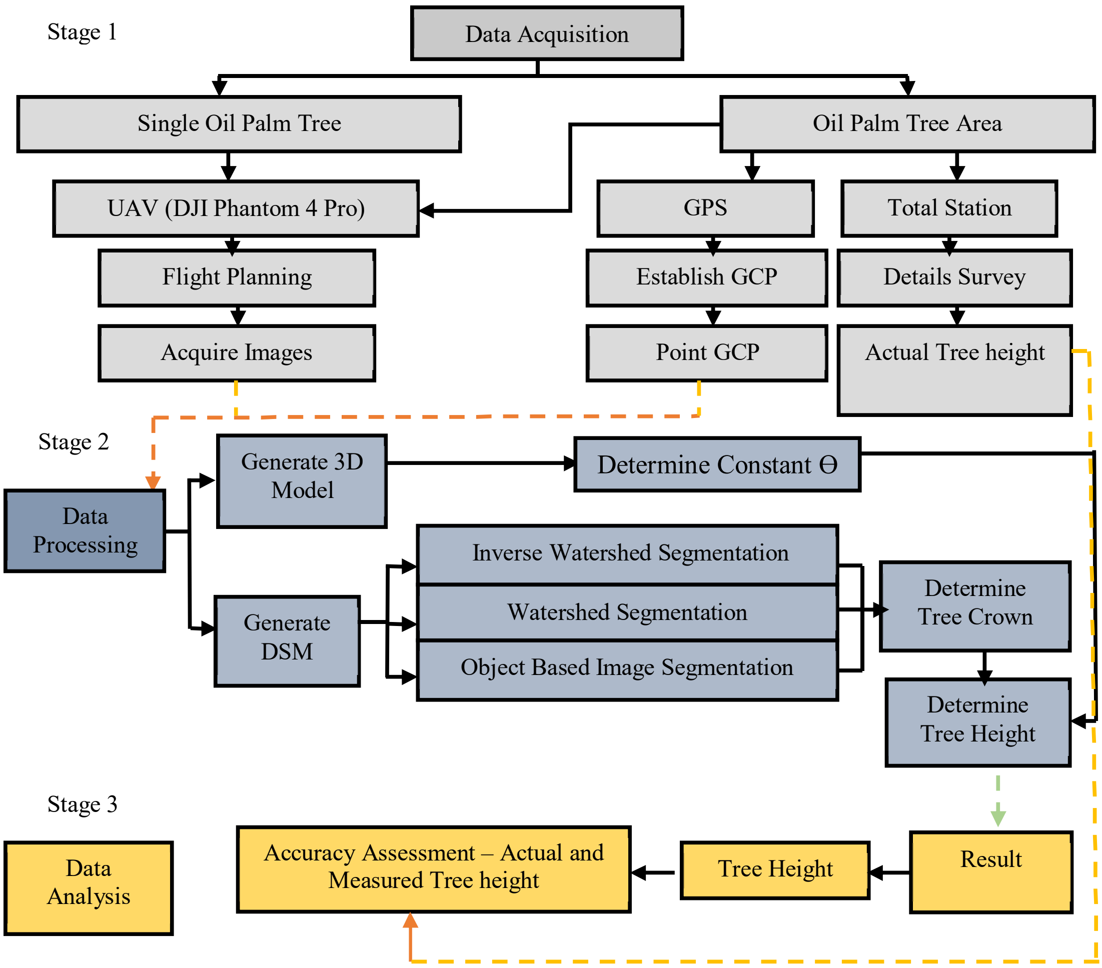

Fig. 1 Research Methodology in Determination Tree Height using UAV Images

The data acquisition was conducted for both the single oil palm tree and oil palm tree plantation in this research. For single oil palm tree, about five single trees (oil palm) were used as simulated models to evaluate the performance and ability of UAV. The single oil palm tree approach aims to identify the constant angle to be used in the formula for calculating tree height. For oil palm tree plantation, the data acquisition was conducted using UAV technology, GPS, and Total station to determine the accuracy of oil palm trees in the research area. In this research, the flying height or altitude of the captured image were taken at different flying heights. The data acquisition for the plantation area is captured at 40m and 60m of flying heights. The differences between these flying heights is based on the circumstances and the nature of the research area.

The single tree approach was carried out to five different single oil palms with 30m of flying altitude and 20m of camera range. The capture mode was configured using time intervals, meaning the image was captured every two seconds with 80 percent overlapping during data acquisition. The resolution of image was calculated automatically based on the flying altitude. In this experiment, the image of single oil palm was captured using point of interest (POI) method or known as oblique imagery. This method is an effective approach for presenting 3D modelling of spatial geographic information. The angle of camera was set at 45 degrees to the object. The images were captured at flying height of 30m for five different location of single tree. From this experiment, the acquired images were processed as a 3D model to estimate the radius of tree crown and tree height values. The tree crown radius and tree height values were estimated by using the 3D model of five single tree. From the estimation values, the constant angle is determined and subsequently to be used for all experiments conducted in simulation and plantation area area. Hence, the constant angle values can be determined by using the specific formula as Eq. 1.

$$Tan\ \theta = \frac{TH}{Radius}$$
$$\theta = \tan^{-1}\frac{TH}{Radius} \quad (1)$$

where: TH = Tree Height Estimation

This experiment obtained five estimation values of tree crown diameters and tree height. However, the angle from the mean measurement is used to approximate the tree height value for the plantation area. From the single tree approach, it was found that an appropriate tree height for capturing the image is in the range of 10 meter to 13 meters. So, this is the basis height to be used for the oil palm plantation area analysis.

As mentioned before, the selection criteria for the research area were the trees with a height range from 10 meters to 13-meters. This criterion was selected based on the results of the single tree approach conducted to determine the constant angle in determining the tree height value. However, the decision of the tree height of oil palm between 10m to 13m in the plantation area was guided by and referred to the plantation officer. The 10-30m can be classified as a mature oil palm tree, and the growth rate normally has stopped. The size of this research area was limited to 200 meters by 200 meters which is equivalent to four (4) hectares.

The oil palm tree plantation area data were acquired at different flying altitudes/heights to determine the effect of photogrammetric results. For this approach, the images were acquired from two different flying heights: 40 meters and 60 meters. The minimum and maximum selection for flying height depended on the safety of UAV usage in the research area during data acquisition.

The initial position of the oil palm tree plantation area was also required to create a flight path by using DJI GS Pro software. Some parameters need to be taken into account before designing the flight path as they can affect image acquisition results [18]. In this research, the flight path of the plantation area was performed using stereo flying mode at different flying heights such as 40m and 60m. The image overlapping was set at 80% for the front, and side lap, which covers an area of 200m by 200m approximately of plantation area determined using Google Earth map.

The data acquisition in the oil palm tree plantation area involved the image acquisition from the nadir angle and the establishment of a ground control point (GCP) at the oil palm plantation area. The UAV was programmed to fly at an altitude of 40 meters and 60 meters above the ground. The images were collected at nadir view (stereo) to take photographs every two seconds. 80% overlapping images for forward and side lap were controlled by pre-programming the automated UAV waypoint flight path. The time for image acquisition was determined based on the requirement of flying altitude and the percentage of image overlapping.

The UAV was programmed to fly and capture images based on the camera settings before take-off, which the values of Ground Sample Distance (GSD) were 1.1cm and 1.6 cm at flight altitudes of 40m and 60m, respectively. The captured images for the plantation area were based on their flying altitude and percentage overlapping sets. For the analysis, the total captured images for the altitudes of 40 meters and 60 meters were recorded at 514 and 312, respectively.

Establishing a Ground Control Point (GCP) is very important to produce a good photogrammetric result accuracy. The GCP is used for the placement and orientation of the UAV aerial photographs in a spatial coordinate system to the real world around it and can improve the relative and absolute accuracy. It is because of the insufficient accuracy of single-frequency GPS for UAVs. Moreover, the aerial triangulation needs to locate photogrammetric block into the coordinate system and the photogrammetric production such as point cloud, DSM, DTM, and orthophoto. GCP is used for data processing and determining map accuracy. In this research, six (6) GCPs were deployed around the research area to georeferenced UAV images. All the GCPs were marked with reflective material for easy identification during a flight mission.

TABLE I
SIX GCPS USED FOR IMAGE PROCESSING

GCP No.	Latitude (deg min sec)	Longitude (deg min sec)	Orthometric Height (m)
GCP1	4°24'19.337"	100°55'49.284"	33.678
GCP2	4°24'22.665"	100°55'46.986"	31.816
GCP3	4°24'12.077"	100°55'45.673"	20.571
GCP4	4°24'14.947"	100°55'45.302"	23.192
GCP5	4°24'15.693"	100°55'42.748"	20.724
GCP6	4°24'17.374"	100°55'44.062"	23.747

Table 1 shows the latitude, longitude, and height value for GCP, selected based on the smallest RMS value using three baselines of reference stations. In addition, to establish the GCP points, the implementation of a detailed survey measurement was required to obtain the actual measurement of oil palm tree height. These measurements were used to validate the measured tree height data with the actual measurement. The actual tree heights were measured using the Topcon ES-105 total station equipment.

In this research, three (3) stations were located near the GCP around the plantation area to obtain the x, y, z values and collect the details of oil palm tree height using a total station. Station 1 was located nearby GCP 3, station 2 nearby GCP 4, and station 3 nearby GCP 6. The 21 selected trees were taken randomly within the research area.

B. Image Processing

In the single tree approach, the image was processed to produce 3D model. The 3D model was used to estimate the constant angle and to determine the tree height based on the algorithm of tree crown delineation. The acquired images were imported and processed using the Agisoft Photoscan software. The photo-alignment process was performed immediately after all the images had been inserted into the software.

Align photos is the process of orientation, finding the camera position for each image, and building a sparse point cloud model. This process consists of sparse reconstruction of 3D geometry by detecting and matching image feature points in the overlapping image. In the single tree approach, the align photo process was implemented for an image captured in different camera views during data acquisition, such as stereo view and the oblique or circle view. In this situation, the image acquired in a circle/oblique camera view was used to produce 3D model and to determine the constant angle.

The next process is building a dense cloud which is used to calculate the depth information for each camera to be combined into a single dense point cloud. This process is based on the estimated camera positions. In this research, the single tree and plantation area approaches were nominated the high quality to perform dense building clouds with aggressive depth filtering during processing. The aggressive depth filter worked well with images that contained actual empty spaces that did not recognize the small surface as a meaningful object and thus generated a hole in the photogrammetry product.

The next process is building a mesh or known as 3D model. Mesh is a geometry that creates a model based on the point cloud. Furthermore, the result of the building mesh can be exported to another format and used to produce a certain analysis. Usually, building mesh is used to generate the 3D model and surface. The surface type selection depends on the object being used and processed for the required application. In this research, the single tree approach is used both surface types, height field, and arbitrary to process build mesh. The arbitrary type was used to perform the 3D model while the height field type produced DSM. The photogrammetric product derived from the build mesh process consists of three (3) types: shaded, solid, and wireframe.

The results of the building mesh are used to perform the build texture process. Build texture is a 3D physical model that reveals the features of surrounding photographs. The model texture can be exported into various formats of 3D models and is useful for creating 3D model. The software creates a photomosaic and places it on the surface of the meshes. In a single tree approach, the selection to produce texture was performed for images captured in stereo and oblique views. The generic mapping model was used to perform texture for oblique camera view image, which this option automatically chose the best photos of meshes into texture, and this mode was preferred for a complicated 3D structures model. Meanwhile, the orthophoto of mapping mode was used to execute the stereo camera view image, which created a photomosaic onto the meshes from the projection plane.

The final process for image processing is building DSM. DSM is widely applied as a significant geospatial information source for various applications. In this single tree approach, DSM was used to perform the tree crown delineation using algorithms. The DSM data was used to determine the tree crown and next to be used to determine the tree height for the single tree approach and plantation area.

In the plantation area approach, aligned photo was implemented from the entire set of images. The images were processed separately at different flying heights, such as 40 meters and 60 meters. The required images were imported into the processing software and proceeded with the same process as in the single tree approach. The accuracy of aligned photo uses a high accuracy and chooses the reference as a preselection for the plantation area. High accuracy uses the full resolution images to identify the same point of each image and match the same point from two or more images. The selection of reference preselection makes the process faster.

The optimization camera was required to obtain a better accuracy of images. This process was performed after aligning photo and marked GCP were completed. All required GCPs were imported into the software. This research used six GCPs to rectify all images with different flying altitudes.

After the dense point cloud has been reconstructed, it is possible to generate a polygonal mesh model based on the dense cloud data by using the build mesh process. The height field of the surface was applied to build the mesh for the plantation area. The next process was building texture. This process was necessary to inspect the texture model before exporting to generate DSM.

Inverse Watershed Segmentation Algorithm (IWS) is one method used to determine the diameter of tree canopy and extract an individual of the tree. In this research, the IWS was implemented by assuming the DSM is a raster surface, which the tree crown is a watershed, and the seed or treetops became a pond. The process steps of IWS used DSM as an input and then smoothing it using a high pass filter. After that proceed to flow direction and create a watershed (hydrology). Then, the watershed in raster format is converted to polygon format, and the tree crown is extracted as the final result. The neighborhood filter was applied to reduce the image noise and adjust the DSM smoothing value in this method. The high pass filter enhanced the boundaries and edge in the raster features. This filter emphasized the comparison between cell values and their neighbors. The flow direction is a tool to determine the characteristics of a surface from every cell in the raster. This tool is used to create individual drainage and to identify the crown delineation in raster layer form. Fig. 2a illustrates the basic steps in the inversed watershed segmentation process.

The Watershed segmentation algorithm is employed due to its role as a powerful segmenting tool that generates a more significant and accurate result of tree crown delineation. However, the local maxima filtering method is used to implement WS algorithm for crown delineation. This method demonstrates the local maxima points that represent the seeds point of treetops within the canopy. The basic step of watershed segmentation also uses DSM as an input. The DSM were filtered by Gaussian filter, which in this research, the setting used for this filter is standard deviation set as 50, kernel types set as the circle, and kernel radius set as 2. After going through the gaussian filter, applying the watershed algorithm, and then proceeding to image classification. The classification is in raster format and was converted to polygon format to determine tree crown diameter. The DSM data was derived from UAV dense cloud, which determined tree crown delineation using watershed segmentation approaches. In this research, the single tree approach applied a Gaussian filter to smoothen the image from the noise and make it fit for analysis and interpretation. The Gaussian filter was used to blur image data and to remove noise and details using the standard deviation.

The Gaussian filter contains three options parameters: standard deviation, kernel radius, and kernel types. The standard deviation parameter smoothens intensity, while the kernel radius parameter controls the number of neighboring data values that are used to calculate the new value of a central grid. The filter has a more emphasized effect in selecting the higher value of the radius parameter. While kernel types parameter consists of two options to identify a matrix of grids in square or circle mode.

Watershed segmentation was implemented to determine the crown delineation of a single tree and oil palm area. The watershed segmentation considered the gray-scale image as a topographic surface. The step of segmentation by watershed was finding the markers and performing a marker-controlled approach due to control over-segmentation. The marker was used to modify the gradient image, and it was a connected component to an image. Crown delineation was conducted using ArcGIS software, and the segmentation of DSM data was added in ArcGIS software to classify and extract the image of the tree crown. Fig. 2b illustrates the basic steps in the watershed segmentation process.

Object Based Image Analysis (OBIA) is an approach where the objects are distinct segments of the image with characteristics of spatial, statistical, and temporal scales. There are two main aspects to OBIA such as segmentation and classification. Homogeneous groups of pixels are identified and form objects or segments with different sizes and shapes (polygons). Fig. 2c illustrates the basic steps in object based image analysis process.

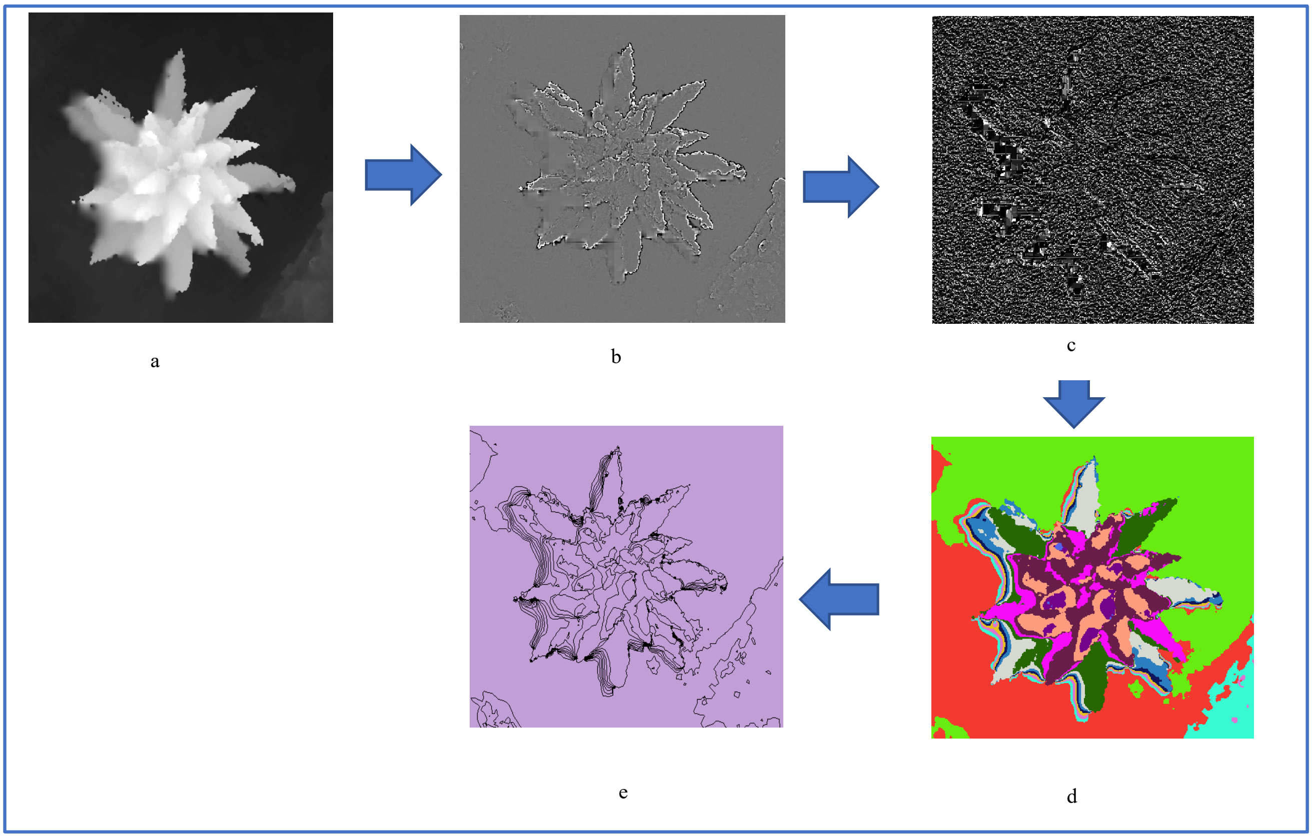

(a)

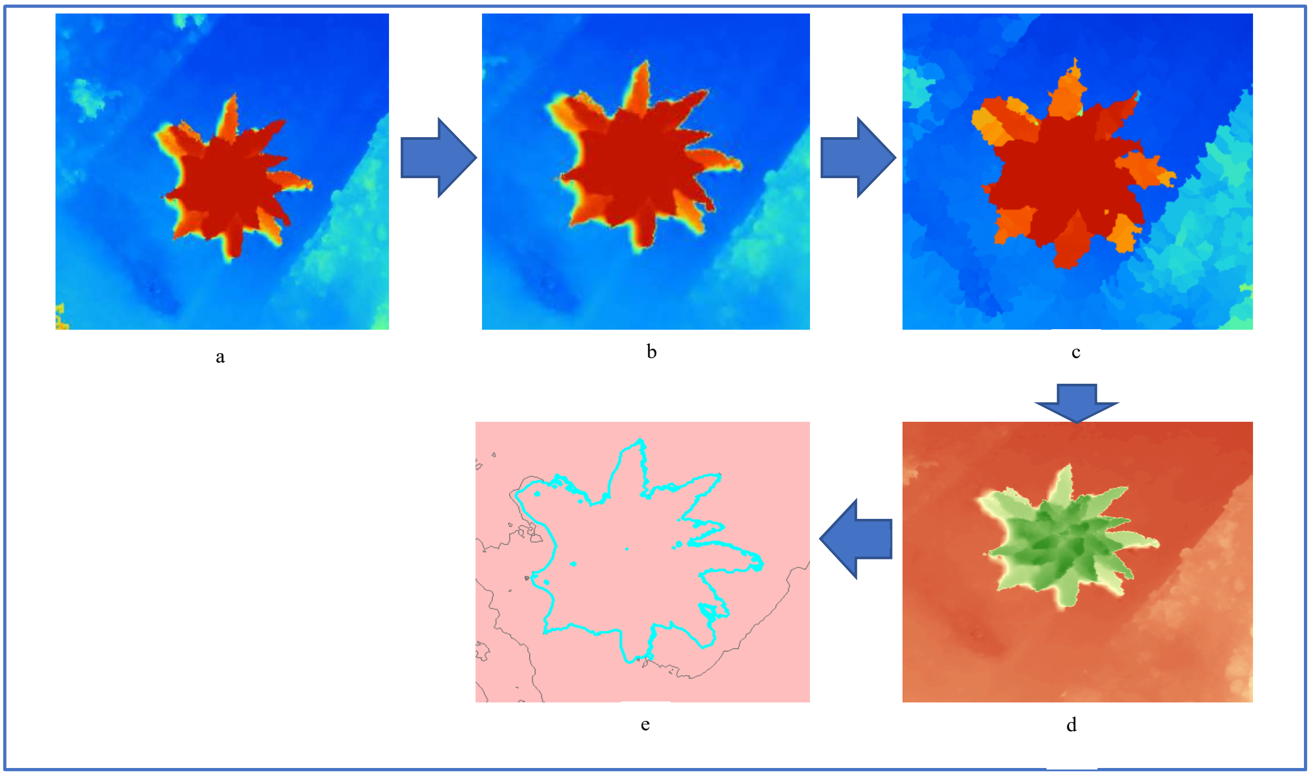

(b)

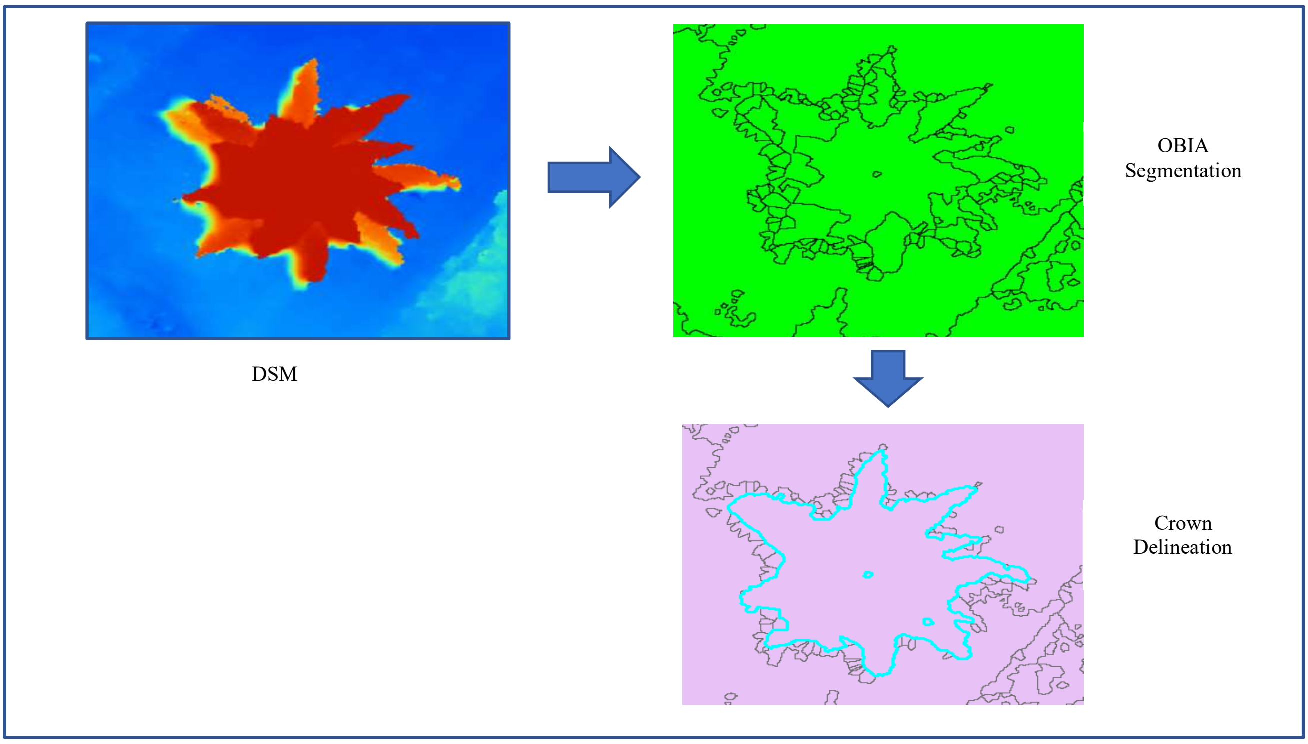

(c)

Fig. 2 Processing; a) IWS Process; a) DSM, b) Smoothing, c) Flow Direction, d) Watershed, e) Raster to Poygon, b) Watershed segmentation process; a) DSM, b) Gaussion filter, c) Segmentation d) Classification, e) Raster to Polygon, c) Object-Based Image Segmentation Process

The determination of tree height was implemented for both the single tree approach and plantation. The data that has been performed with segmentation was converted to vector data format. Further, the overlay process was performed for segmentation data with tree crown data. The tree crown shape was obtained from digitizing the crown based on the orthophoto data. In a plantation area, the overlay process is performed to combine two input map layers as one layer of the spatial and attribute data.

In such a process, every polygon of a layer is combined in pairs with that of another layer. The DSM and tree crown data were combined using the overlay process in this research. In order to determine the area of the tree crown, the dissolving process is used to group based on specified attributes. This process can be statistical data of the tree crown area. In this research, the tree crown area was required to calculate the tree crown diameter. Therefore, the overlay and dissolution process was necessary to obtain the tree crown area. As a result of the overlay and dissolve process, the value of tree crown diameter was determined by using Eq. 2.

$$CD = \sqrt{\left[\frac{4*area}{\pi}\right]} \tag{2}$$

Where,
CD = Crown Diameter
π = 3.142

The calculations process is performed since all the data is converted to a vector data format. This research required the constant angle value to determine tree crown and tree height using Eq. 2. Angle (theta) was obtained from the 3D model estimation measurement of crown diameter and height of a single oil palm using Agisoft Photoscan. The 3D model of five single oil palm trees was used to estimate crown diameter and tree height. Hence, measurement estimation reading was taken four times for 3D crown diameter and 3D tree height. The crown diameter measurement for every single tree was calculated beforehand. In this research, the size of tree crown diameter was measured four times for the five single oil palm trees. The crown diameter measurement needed to be summed up and divided into four to obtain the actual result. Usually, more than two diameter measurements or crown diameter assessments may be taken and averaged. The basic calculation was used to determine the angle of the triangle based on the estimated crown diameter and tree height value. The final five radius and tree height values are used to calculate angle θ.

The measurement is required to determine the diameter of the tree crown. The circle diameter, like a projection of a tree crown, is important to be identified, in which it is overlaid with those manually produced from the orthophoto. However, the raster image cannot be used directly to obtain the statistical value of tree crown diameter. So, the conversion process was applied to convert the raster image to the polygon. The characteristics of oil palm, such as area of shape, length of shape, and classification of the polygon, are shown in the attribute table. The diameter of the oil palm is calculated based on Eq. 3. From that, the calculation of tree height was obtained based on the result of crown diameter, and the calculation was applied by using Eq. 3.

$$TH = (CD/2) * \tan\theta \tag{3}$$

Where,
TH = Tree Height
CD = Crown Diameter

Based on Eq. 3, the tree crown diameter and the angle value must be calculated in order to obtain the tree height value. The overlay process was performed between the crown circle and the segmented data. Meanwhile, the segmented data was obtained from the segmentation process using three algorithms. This process organizes the spatial in multiple data layers and gathers attributes from the source dataset. After that, the dissolving process is performed, which is the aggregation consisting of polygons that share the same category or code. In this research, the dissolving process was used to combine the polygon of the crown circle that has been overlaid and considered the highest pixel values for the tree height determinant.

III. Result and Discussion

Table 2 shows the tree crown value derived from the field calculator tool. As shown in the single tree approach, all the algorithms have also been used in the plantation area. The determination of tree crown for plantation area was rendered by algorithms such as IWS, WS, and OBIA. However, the tree crown shape used the same circle for all algorithms and used for different flying heights. In this research, the canopy distance between trees is an element affecting the performance of the algorithm method. Table 2 shows the tree crown diameter obtained from different algorithm.

TABLE II
Tree Crown Diameter

Flying Height (m)	**Tree Crown Diameter (meter)**		
	IWS	WS	OBIA
40	8.960	9.746	8.561
60	8.937	9.048	8.634

Table 2 shows the difference between tree crowns is about a centimeter to meter level. These results are due to the outcome of the segmentation processing for each algorithm. The result of the tree crown was used to determine the tree's radius, and then it can be used for tree height calculation. Based on Fig. 3, the result shows the tree crown determinant, which used the IWS, WS and OBIA algorithms at different flying heights. The crown diameter values obtained from all algorithms indicated the difference in the values between 4.817m to 11.106m at different flying heights.

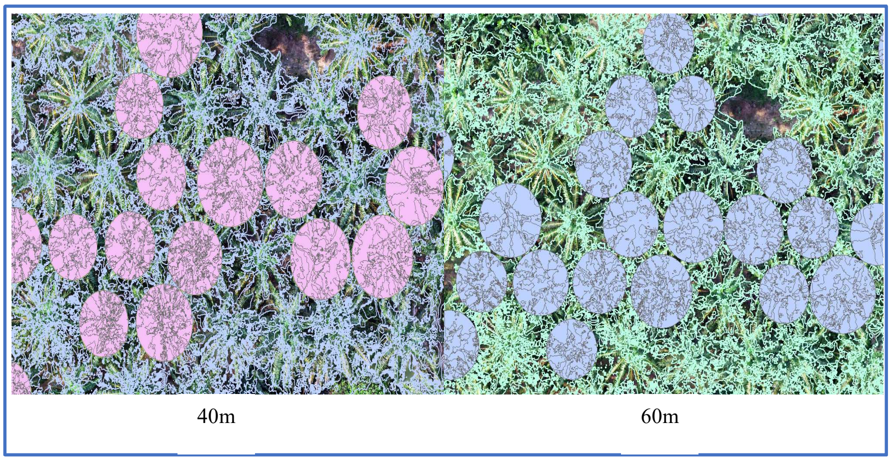

(a)

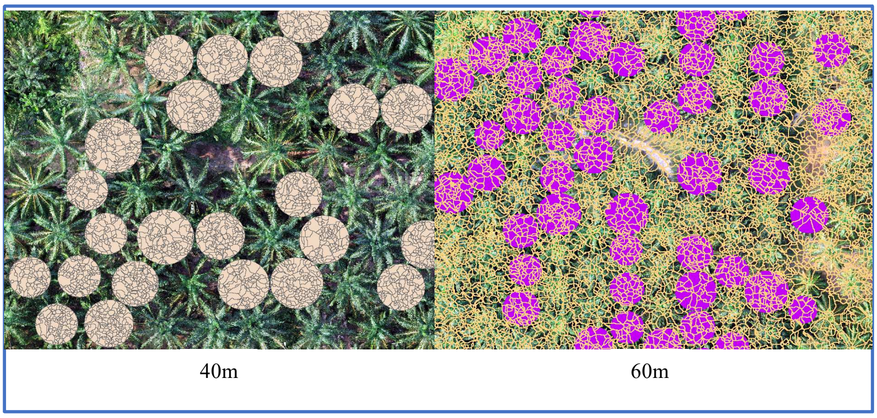

(b)

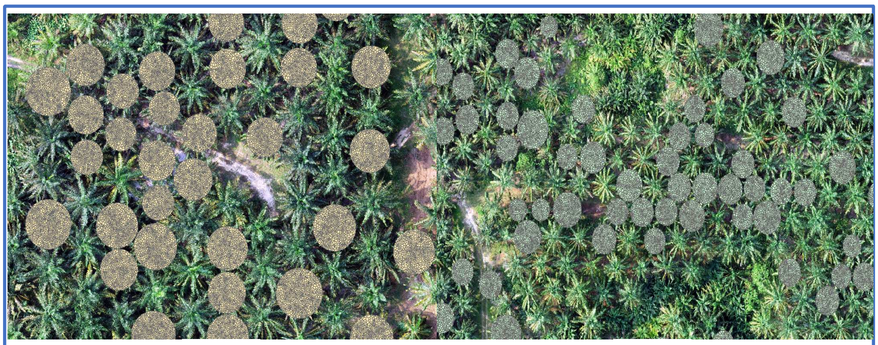

(c)

Fig. 3 Results from different altitudes; a)IWS, b) WS, c) OBIA

Based on the result shown, all algorithms used have achieved the objective of obtaining the tree crown result for the plantation area. The result obtained was also dependent on the surrounding parameters of the plantation area. The tree crown result obtained from all these algorithms was used to determine the tree height value. The calculated tree height for all algorithms described in Table 3.

TABLE III
TREE HEIGHT OBTAINED FROM ALL ALGORITHMS

Point	Watershed Algorithm (WS)		Object-Based Image Analysis Algorithm (OBIA)		Inverse Watershed Algorithm (IWS)		Actual Trees (m)
	60m	40m	60m	40m	60m	40m	
1	21.184	21.655	21.069	20.951	21.721	22.310	20.976
2	22.823	21.682	22.507	21.448	23.107	21.834	21.876
3	22.677	22.566	21.802	21.985	22.777	22.984	21.898
4	22.367	23.123	22.063	22.615	22.291	23.731	22.201
5	24.346	23.822	24.099	23.687	24.369	23.810	23.841
6	23.188	23.572	22.900	23.299	23.870	23.445	22.981
7	24.643	24.399	24.220	24.147	25.302	24.356	24.137
8	26.196	27.493	25.808	27.078	26.994	28.118	26.350
9	25.648	25.301	25.062	24.801	26.260	25.738	24.740
10	23.352	23.534	23.321	23.221	23.542	24.263	23.186
11	25.451	25.046	24.839	24.795	26.013	25.539	24.345
12	22.319	22.376	22.523	22.267	23.143	24.492	21.520
13	22.254	22.427	22.124	21.847	22.008	22.948	21.826
14	21.474	21.425	21.481	21.228	22.178	22.821	20.804
15	23.068	21.916	22.658	21.511	23.070	21.512	21.975
16	22.182	21.326	21.608	20.857	22.374	21.835	21.187
17	20.687	19.904	20.416	19.435	20.813	20.792	19.928
18	20.667	19.772	20.427	19.499	20.986	20.074	19.887
19	22.935	23.524	22.547	23.210	23.655	24.110	22.734
20	23.240	23.101	22.956	22.936	23.791	23.504	22.937

The data in Table 3 were used to calculate the error for each algorithm from different altitudes. The error plot for all algorithms is illustrated in Fig. 4. Fig. 4a shows that the 40m and 60m data from the WS algorithm has an undulated pattern that ranges about $\pm$1.2m. The Residual Mean Square Error (RMSE) was used to calculate measured tree height accuracy. The RMSE formula uses the actual tree height data to calculate the measured data with the actual data. The RMSE for WS algorithm for 40m is about $\pm$0.671m, and 60m is about $\pm$0.575m. Fig. 4b shows the 40m and 60m data from the OBIA algorithm has undulated pattern that ranges about $\pm$1.5m. The RMSE for OBIA for 40m is about $\pm$0.444m and $\pm$0.381m. Fig. 4c shows the 40m and 60m data from the IWS algorithm has undulated pattern that ranges about $\pm$3.4m for 40m altitude and $\pm$1.6m for 60m altitudes. The RMSE for IWS for 40m is about $\pm$1.040m and $\pm$1.226m.

Therefore, based on these analyses, it was found that the OBIA algorithm has the best accuracy among the three algorithms. It is followed by WS algorithm and then the IWS algorithm. The OBIA algorithm can give an accuracy about 0.444m at 40m and 0.381m at 60 altitudes. The accuracy for WS and OBIA stated that the 60m altitude gives the better accuracy compared to 40m altitude. However, the IWS gives the vice versa result.

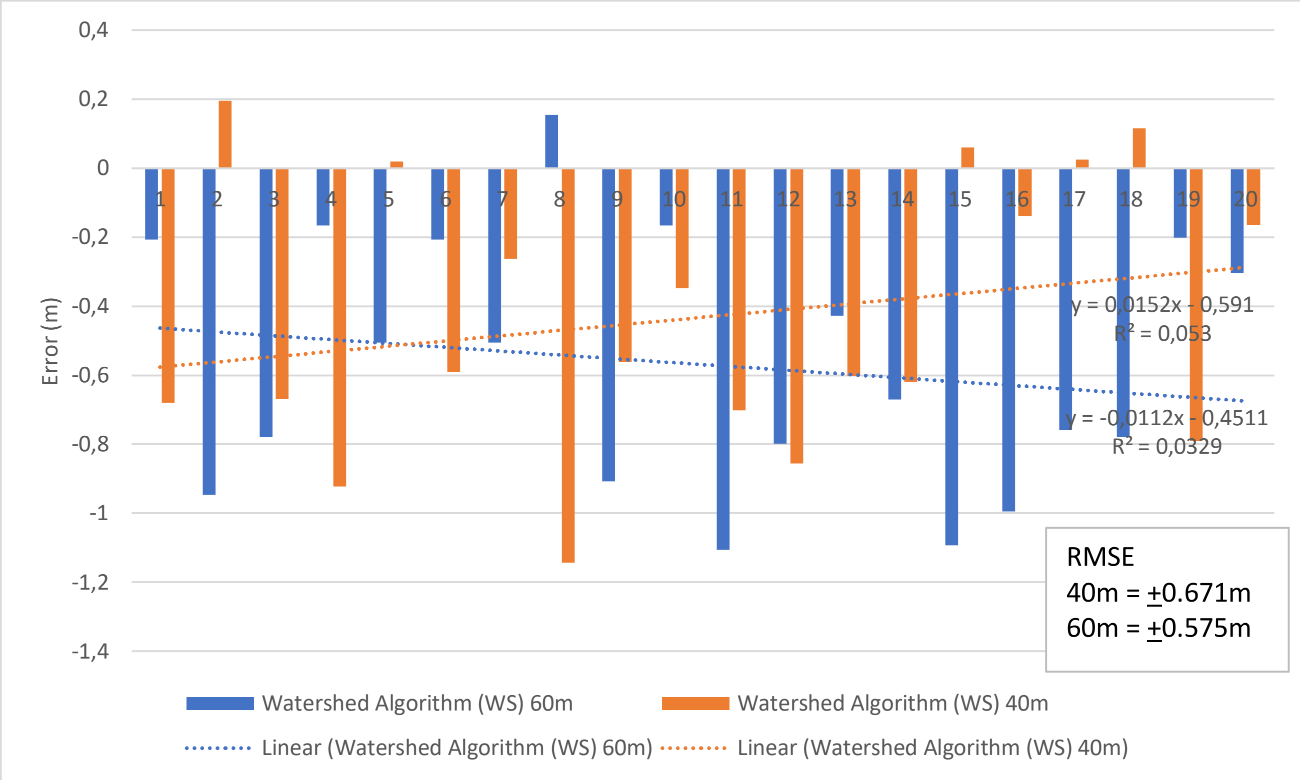
0,4
0,2
0
-0,2
-0,4
-0,6
-0,8
-1
-1,2
-1,4
Error (m)
1 2 3 4 5 6 7 8 9 10 11 12 13 14 15 16 17 18 19 20
y = 0,0152x - 0,591
R² = 0,053
y = -0,0112x - 0,4511
R² = 0,0329
RMSE
40m = ±0.671m
60m = ±0.575m
Watershed Algorithm (WS) 60m
Watershed Algorithm (WS) 40m
Linear (Watershed Algorithm (WS) 60m)
Linear (Watershed Algorithm (WS) 40m)

(a)

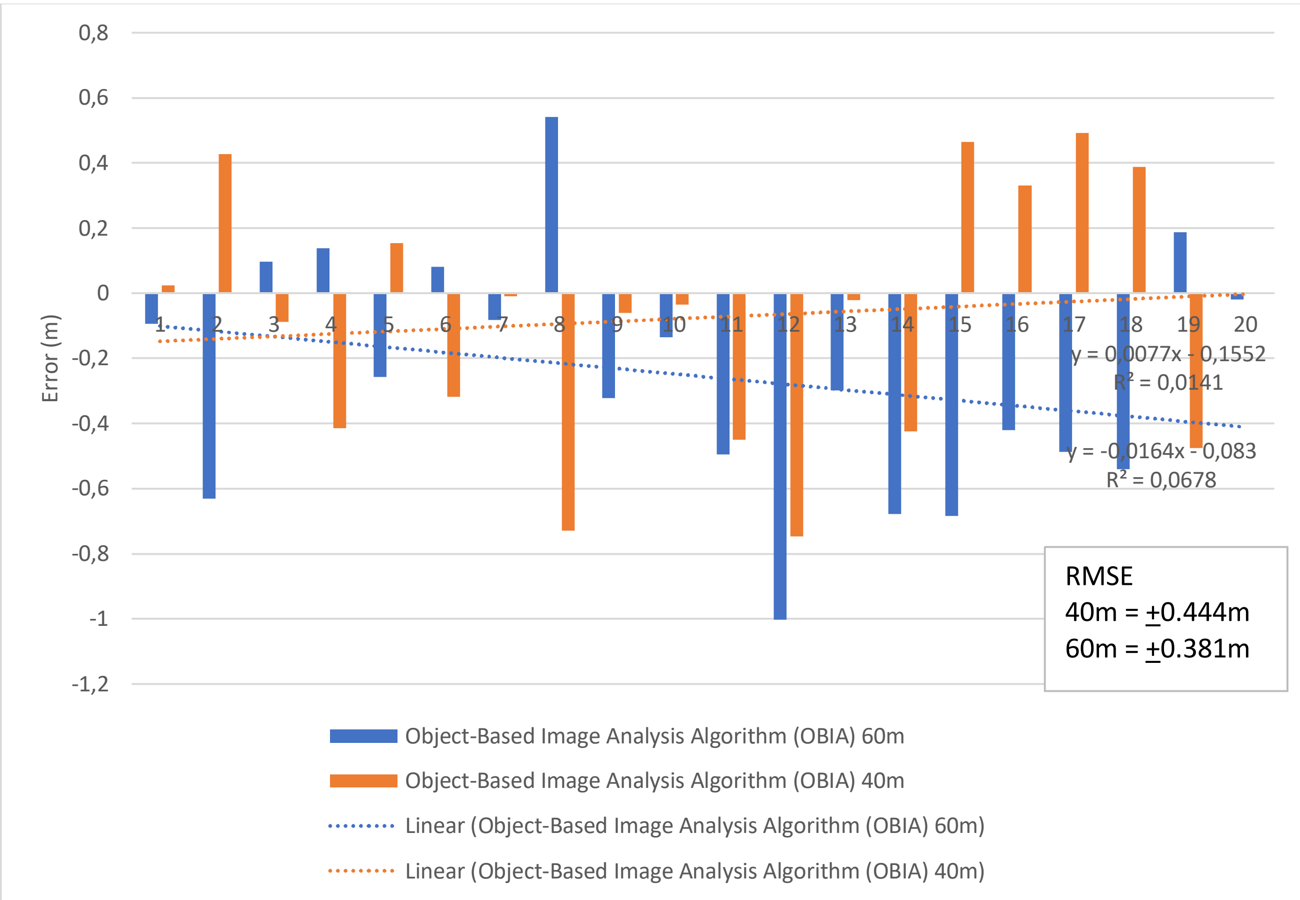
0,8
0,6
0,4
0,2
0
-0,2
-0,4
-0,6
-0,8
-1
-1,2
Error (m)
1 2 3 4 5 6 7 8 9 10 11 12 13 14 15 16 17 18 19 20
y = 0,0077x - 0,1552
R² = 0,0141
y = -0,0164x - 0,083
R² = 0,0678
RMSE
40m = ±0.444m
60m = ±0.381m
Object-Based Image Analysis Algorithm (OBIA) 60m
Object-Based Image Analysis Algorithm (OBIA) 40m
Linear (Object-Based Image Analysis Algorithm (OBIA) 60m)
Linear (Object-Based Image Analysis Algorithm (OBIA) 40m)

(b)

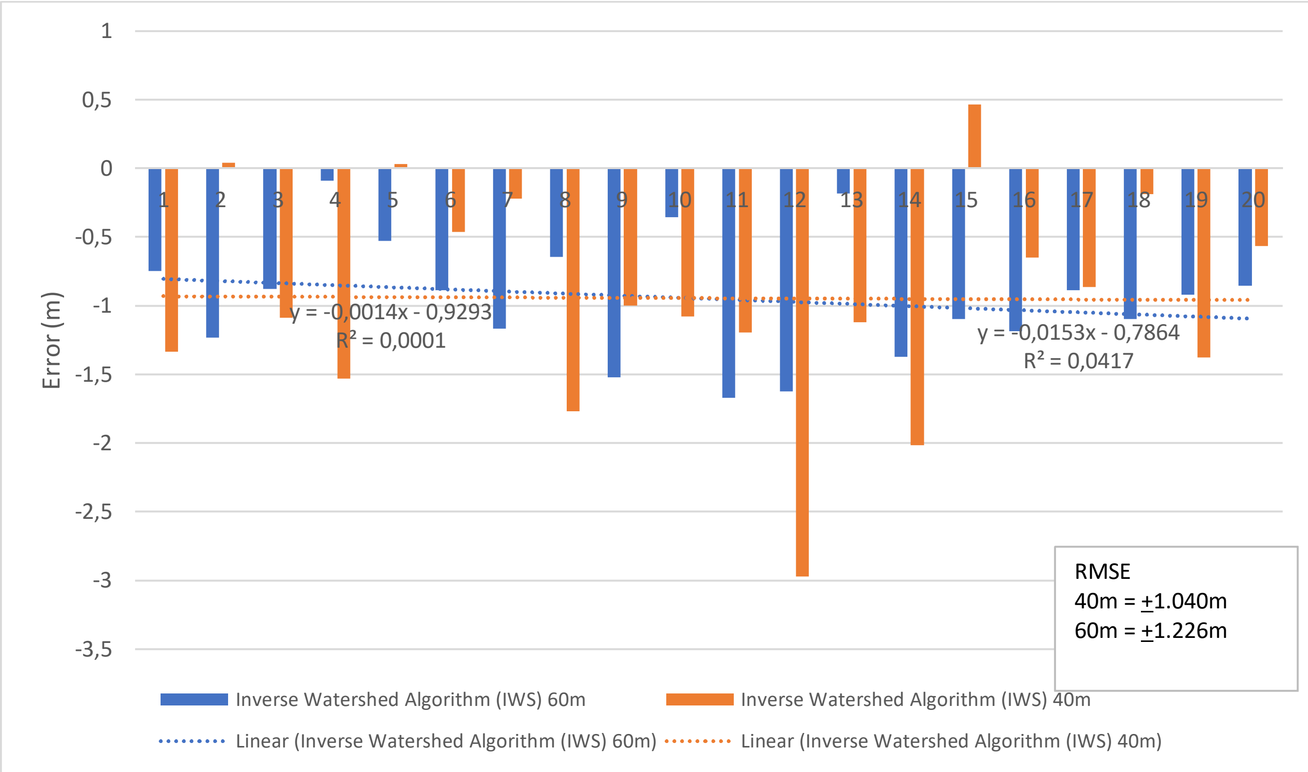

(c)

Fig. 4 Error pattern; a) WS algorithm, b) OBIA, c) IWS

IV. Conclusion

In conclusion, this research has performed tree crown was delineated from three different algorithms: watershed segmentation (WS), object-based image analysis (OBIA), and inverse watershed segmentation at different altitudes or flying heights. The exploratory research which was conducted on a single tree approach involved only a single oil palm tree. The single oil palm data was acquired using UAV at different flying heights of 40m, and 60m. This experiment was conducted to determine the constant angle of tree height from the tree crown. It was found that among these three algorithms, OBIA gave the best method to determine the tree height of the plantation canopy area due to the accurate result. The methods and algorithms used in this research were recognized, and the algorithms were proven successful in determining the tree height values. By completing the experiment, it was confirmed that the proposed algorithms were appropriate for estimating the tree height at different flying heights.

Acknowledgment

Faculty of Architecture, Planning, and Surveying Universiti Teknologi MARA (UiTM) is greatly acknowledged for enabling this research to be carried out. The authors would also like to thank the directly or indirectly involved in this research.

References

[1] M. Wang and J. Lin, "Retrieving individual tree heights from a point cloud generated with optical imagery from an unmanned aerial vehicle (UAV)," *Canadian Journal of Forest Research*, vol. 50, no. 10, 2020.

[2] S. Krause, T.G. Sanders, J.P. Mund and K. Greve, "UAV-based photogrammetric tree height measurement for intensive forest monitoring," *Remote Sens*., vol. 11: 758, 2019.

[3] F. Giannettia, N. Puletti, P. Stefano, D. Travaglinia and G. Chiricia, "Assessment of UAV photogrammetric DTM-independent variables for modelling and mapping forest structural indices in mixed temperate forests," *Ecol. Indic*., vol. 117: 106513, 2020.

[4] H. Huang, S. He and C. Chen, " Leaf abundance affects tree height estimation derived from UAV images," *Forests*, vol. 10: 931, 2019.

[5] C. Barnes, H. Balzter, K. Barrett, J. Eddy, S. Milner and J.C. Suárez, "Individual Tree Crown Delineation from Airborne Laser Scanning for Diseased Larch Forest Stands," Remote Sensing, vol. 9, no. 3, pp. 1–20, 2017.

[6] M. Vastaranta, M. Holopainen, M. Karjalainen, V. Kankare, J. Hyyppa and S. Kaasalainen, "TerraSAR-X Stereo Radargrammetry and Airborne Scanning LiDAR Height Metrics in Imputation of Forest Aboveground Biomass and Stem Volume," IEEE Transactions on Geoscience and Remote Sensing, vol. 52, no. 2, pp. 1197–1204, 2014.

[7] E.G. Parmehr and M. Amati, "Individual Tree Canopy Parameters Estimation Using UAV-Based Photogrammetric and LiDAR Point Clouds in an Urban Park," *Remote Sensing*. 2021, vol. 13, no. 11, 2062, 2021.

[8] L. Cao, H. Liu, X. Fu, Z. Zhang, X. Shen and H. Ruan, "Comparison of UAV LiDAR and Digital Aerial Photogrammetry Point Clouds for Estimating Forest Structural Attributes in Subtropical Planted Forests," *Forests,* vol. 10, 145, 2019.

[9] T. Swinfield, J.A. Lindsell, J.V. Williams, R.D. Harrison, Agustiono, Habibi, E. Gemita, C.B. Schönlieb and D.A. Coomes, "Accurate Measurement of Tropical Forest Canopy Heights and Aboveground Carbon Using Structure From Motion," *Remote Sens*., vol. 11, 928, 2019.

[10] S. Ganz, Y. Käber and P. Adler, "Measuring Tree Height with Remote Sensing—A Comparison of Photogrammetric and LiDAR Data with Different Field Measurements," *Forests*, 2019, vol. 10, no. 8, 694, 2019.

[11] L. Jurjević, X. Liang, M. Gašparović and I. Balenović, "Is field-measured tree height as reliable as believed – Part II, A comparison study of tree height estimates from conventional field measurement and low-cost close-range remote sensing in a deciduous forest, *ISPRS Journal of Photogrammetry and Remote Sensing*, Vol. 169, pp. 227-241, 2020.

[12] M. Koeva, M. Muneza, C. Gevaert, M. Gerke, F. Nex, M. Koeva, F. Nex, "Using UAVs for Map Creation and Updating. A Case Study in Rwanda," *Survey Review*, vol. *50*, no. 361, pp. 312–325, 2018.

[13] L. Huo and E. Lindberg, "Individual tree detection using template matching of multiple rasters derived from multispectral airborne laser scanning data," *International Journal of Remote Sensing*, vol. 41, no. 24, pp. 9525-9544, 2020.

[14] A.C. Birdal, U. Avdan and T. Türk, "Estimating Tree Heights with Images from An Unmanned Aerial Vehicle," *Geomatics, Natural Hazards and Risk*, vol *8*, no. 2, pp. 1144–1156, 2017.

[15] L. Won-Jin and L. Chang-Wook, "Forest Canopy Height Estimation Using Multiplatform Remote Sensing Dataset," *Journal of Sensors*, vol. *2018*, no. 9, 2018.

[16] K.N. Tahar, M.A. Asmadin, S.A. Sulaiman, N. Khalid, A.N. Idris and M. H. Razali, "Individual Tree Crown Detection Using UAV Orthomosaic," *Engineering, Technology & Applied Science Research*, vol. 11, no. 2, pp. 7047-7053, 2021.

[17] Y. Wang, M. Lehtomäki, X. Liang, J. Pyörälä and A. Kukko, "Is Field-Measured Tree Height As Reliable As Believed – A Comparison Study of Tree Height Estimates from Field Measurement , Airborne Laser Scanning and Terrestrial Laser Scanning In a Boreal Forest," *ISPRS Journal of Photogrammetry and Remote Sensing*, vol. *147*, no. 201, pp. 132–145, 2019.

[18] K. Zhao, J.C. Suarez, M. Garcia, T. Hu, C. Wang and A. Londo, "Utility of Multitemporal LiDAR for Forest and Carbon Monitoring: Tree Growth, Biomass Dynamics, and Carbon Flux," *Remote Sensing of Environment*, vol. *204*, 883–897, 2018.

[19] X. Zhuo, T. Koch, F. Kurz, F. Fraundorfer and P. Reinartz, "Automatic UAV Image Geo-Registration by Matching UAV Images to Georeferenced Image Data," *Remote Sensing*, vol. *9*, no. 4, pp. 1–25, 2017.

[20] A.P. Colefax, P.A. Butcher and B.P. Kelaher, "The Potential for Unmanned Aerial Vehicles (UAVs) to Conduct Marine Fauna Surveys in Place of Manned Aircraft," *ICES Journal of Marine Science*, vol. *75*, no. 1, pp. 1–8, 2018.